Communications in Computational Chemistry
Commun. Comput. Chem., Vol. 7, No. 2, 145–151
doi: 10.4208/cicc.2025.49.01
Regular Article

DFT Study on the Mechanism of Water Oxidation Catalyzed by a Mononuclear Copper Complex

Zhi-Bo Yang[1], Xin Lu[1], Miao-Miao Li[1], Han-Xiao Guo[1], Si-Xiang Chen[1],

Rong-Zhen Liao[2] and Ying-Ying Li[1,*]

[1]School of Chemistry and Chemical Engineering, Henan Engineering Technology Research Center for Green Catalytic and Atom Economic Conversion of Coal-based Benzene, Zhengzhou Normal University, Zhengzhou 450044, China;

[2]Key Laboratory of Material Chemistry for Energy Conversion and Storage, Ministry of Education, Hubei Key Laboratory of Bioinorganic Chemistry and Materia Medica, Hubei Key Laboratory of Materials Chemistry and Service Failure, School of Chemistry and Chemical Engineering, Huazhong University of Science and Technology, Wuhan 430074, China

[*] Corresponding authors: liyingying@zznu.edu.cn

Received on 20 February 2025; Accepted on 11 May 2025

Abstract: This work employed DFT calculations to elucidate the mechanism of water oxidation reaction catalyzed by a mononuclear pyridine-based copper complex, which was reported to be a homogeneous water oxidation catalyst in a pH=11.84 buffer solution. The coordination of one water molecule with the Cu^{II} center leads to the generation of the Cu^{II}-OH_2 (**1-H_2O**). The active species (Cu^{IV}=O, **3**) is generated after two subsequent proton-coupled electron transfer processes from **1-H_2O**. **3** triggers the O-O bond formation via water nucleophilic attack mechanism. The triplet O_2 can be released after following two oxidation processes. The formation of the O-O bond is the rate-determining step for the catalytic cycle associated with a total barrier of 19.3 kcal/mol.

Key words: water oxidation, density functional calculations; reaction mechanism, copper complex.

1. Introduction

Solar energy is an ideal source of energy. However, obtaining and utilizing solar energy is a challenge. Inspired by nature, a promising approach is to construct artificial photosynthetic systems [1]. The water oxidation reacti on, consisting of the releasing of four protons and four electrons as well as the O-O bond formation process (equation **1**), lies at the heart of this system. The oxidation potential of the water oxidation reaction is 1.23 V at pH 0. This oxidation reaction is both thermodynamically and kinetically very difficult. It is necessary to develop efficient water oxidation catalysts (WOCs).

$$2H_2O\,(aq) \longrightarrow O_2(gas) + 4e^- + 4H^+(aq) \quad (E_0 = 1.23\ V - 0.059\ pH) \quad (1)$$

Homogeneous WOCs have the advantages of mechanism study and tunable ligand design [2]. The development of WOCs dates back to the design of the "blue dimer" in 1982 [3]. Since then, some Ru and Ir-based WOCs have been reported [4-7]. However, non-noble and earth-abundant metal-based complexes [8], such as Fe [9,10], Co, [11-14] Ni [15], Cu [16], V [17], Mn [18,19] based complexes, have

been drawing more and more attention in terms of the application in industry. Computational chemistry is useful for detailed mechanism research, which is beneficial for the design of more efficient WOCs. Great progress has been made in the computational community for the mechanism study of water oxidation reaction, [20-28] including the theoretical mechanism study of Cu-based WOCs [29-33].

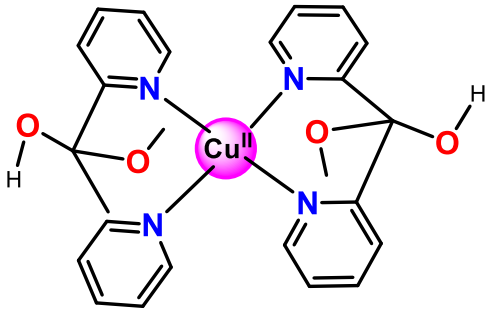

Scheme 1. Schematic structure of the copper complex.

In 2021, a copper complex (**Scheme 1**) was reported to be a water oxidation catalyst in sodium acetate buffer solution at the pH of 11.84 with a reported TOF of 9.20 s^{-1}.[34] The complex adopts a square-planar geometry, and four pyridyl nitrogen atoms coordinate with the Cu^{II} center. Two oxygens from the OCH_3 groups occupy axial positions above and below the plane but do not directly coordinate with the copper center. The linear relationship between the concertation of the catalyst and the catalytic current peaks was disclosed, which indicates a first-order reaction.[34] The reaction mechanism remains unclear. In the present work, DFT calculations were used to investigate the reaction mechanism of water oxidation catalyzed by the copper complex. The oxidation process, O-O bond formation and the release of the O_2 were calculated.

2. Theoretical method

The Gaussian 16 program was used to do all calculations [35]. B3LYP-D3 functional was employed to do geometrical optimizations [36,37]. 6-31G(d,p) basis set was used to describe non-mental elements, while SDD pseudopotential was employed for Cu element [38]. The analytic frequency calculations were carried out to confirm the nature of all structures at the same level. Single-point calculations with the SMD implicit solvation model were carried out to obtain the final energy, where 6-311+G(2df,2p) was used to describe all non-mental elements [39].

A reference potential of 1.5 V (vs. SHE) was used to construct the Gibbs energy diagram since the controlled potential electrolysis experiment was tested at the potential of 1.5 V [34]. The absolute potential of 4.281 V of SHE was token as a reference [40]. The pK_a values of various intermediates were calculated to study the proton-releasing process. The proton solvation energy of -264.0 kcal/mol in water from the experimental study was used. The pK_a values were used to determine whether the oxidation process involved proton release. For an oxidation process, the high oxidation intermediate prefers to be deprotonated if its pK_a is lower than the pH of the reaction solution. Under such conditions, the oxidation process is coupled with the release of a proton. The solvation energy (-6.3 kcal/mol) of water in aqueous was used [41]. A concentration correction value of 1.9 kcal/mol (RTln24.5) at 298.15K was applied to all species to account for the standard state changes arising from the use of the SMD solvation model. This correction originates from the calculation of the solvation energy in aqueous solution that defined as the free energy of transfer of the solute from the gas phase (24.5 L mol^{-1}) to the aqueous phase (1 mol L^{-1}). Meanwhile, water has a concentration correction term of 4.3 kcal/mol. The SCF convergence was set to 10^{-8}. The computational methodology employed in the present work has been validated for mechanistic investigations of water oxidation reactions.

3. Results and discussion

3.1 The oxidation process

The DFT calculations commenced from the geometry optimization of the Cu catalyst (**1**). The optimized structure is displayed in **Figure 1**. **1** is a doublet state. The copper center is in a +2 oxidation state. Four nitrogen atoms from pyridines coordinate with the Cu^{II} center at a distance of 2.04 Å, which is consistent with the reported value of 2.007/2.000 Å [34]. Two oxygen atoms of the two methanol groups have distances of 2.51 Å away from the metal center. The spin density on Cu is 0.62. To initiate the water oxidation reaction, at least one water molecule must coordinate with the Cu^{II} center. The coordination of one water with the Cu^{II} leads to the generation of **1-H_2O** (**Figure 1**.) This step was calculated to be endergonic by 7.0 kcal/mol (**Figure 2**). The coordination of the water with the copper center resulted in the release of one N atom from the metal coordination sphere. The Cu-O1 distance was calculated to be 2.00 Å in **1-H_2O**. The second water combined with the metal in **1-H_2O** is thermodynamically unfavorable, as the coordination of the second water to **1-H_2O** is endergonic by 11.3 kcal/mol (**Figure S1**). In addition, the one-electron oxidation of **1** has a calculated redox potential of 2.2 V, suggesting the oxidation of **1** is unlikely (**Figure S1**).

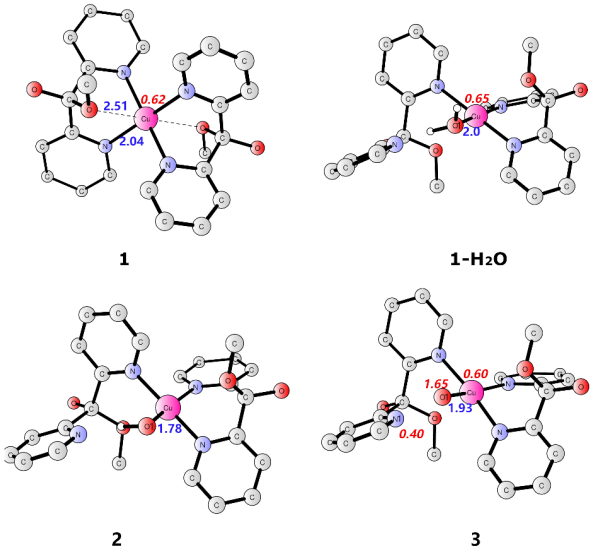

Figure 1. Optimized structure of **1** (doublet), **1-H_2O**(doublet), **2**(singlet) and **3**(quartet). Spin densities on selected atoms are shown in red in italics. Distances are shown in blue in Å. Unimportant H atoms are not shown.

The pK_a of $\mathbf{2_{pt}}$ (the protonation state of **2**, Cu^{III}-OH_2, Figure **S1**) was calculated to be 3.3, suggesting that the deprotonation state domains in the pH=11.84 solution. Therefore, the first oxidation of **1-H_2O** is associated with a proton release from the water ligand. This is

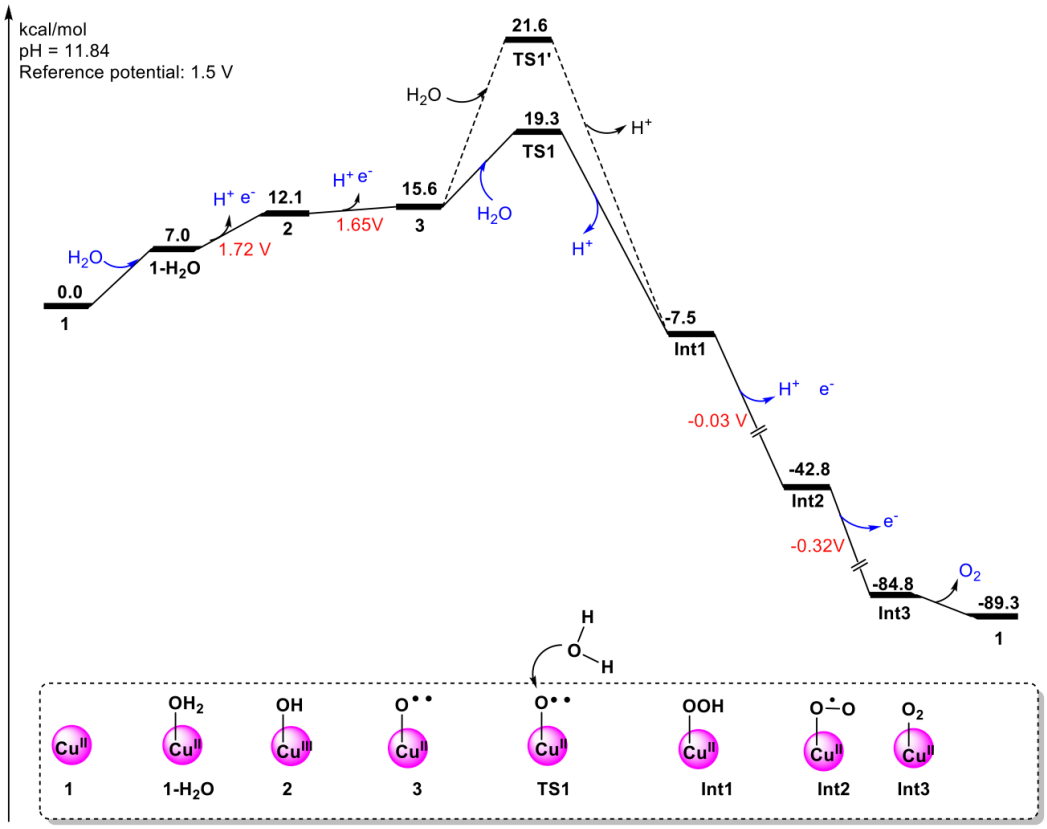

Figure 2. Energy diagram of the catalyzed water oxidation reaction.

consistent with the experimental study that the onset potential for water oxidation has a pH-dependence slope of 53 mV pH^{-1}.[34] This oxidation process generates **2** (**Figure 1**, Cu^{III}-OH). **2** prefers to be singlet, while the triplet is 3.7 kcal/mol higher. The Cu-O1 has a distance of 1.78 Å in **2**. For the triplet state, the spin densities on Cu, O1, and ligand are 0.63, 0.67, and 0.40, respectively. (**Figure S1**) This indicates that the release of the first electron from the copper center is energetically more favorable than its release from the ligand. This oxidation process proceeds at a potential of 1.72 V. When a reference potential of 1.5 V is applied, this process is endergonic by 5.1 kcal/mol (**Figure 2**).

3 (**Figure 1**, formal Cu^{IV}=O) was generated after a second proton-coupled electron transfer process. The $\mathbf{3_{pt}}$ (the protonation state of **3**, Cu^{IV}-OH, **Figure S1**) has a pK_a of 0.10. **3** is a quartet, while the doublet lies at + 2.6 kcal/mol above the ground state. The Cu-O1 distance is 1.93 Å in **3**. For the quartet, the spin densities on Cu, O1, and N1 are 0.60, 1.65, and 0.40, respectively, suggesting the formation of a Cu^{II}-oxygen diradical species. In the doublet state, the calculated spin densities are -0.64 on Cu, 1.46 on O1, and 0.41 on N1. (**Figure S1**) The spin population indicates the occurrence of the intramolecular electron transfer during the oxidation from **2** to **3**. The redox potential of this oxidation process was calculated to be 1.65 V, indicating that this process is slightly endergonic by 3.5 kcal/mol with an applied reference potential of 1.5 V (**Figure 2**). One thing that should be considered here is whether the OH group is protonated. The calculated pK_a of 14.6 of **3** suggests the protonation state is more favorable. (**Figure S2**)

3.2 The O-O bond formation and the release of the O_2

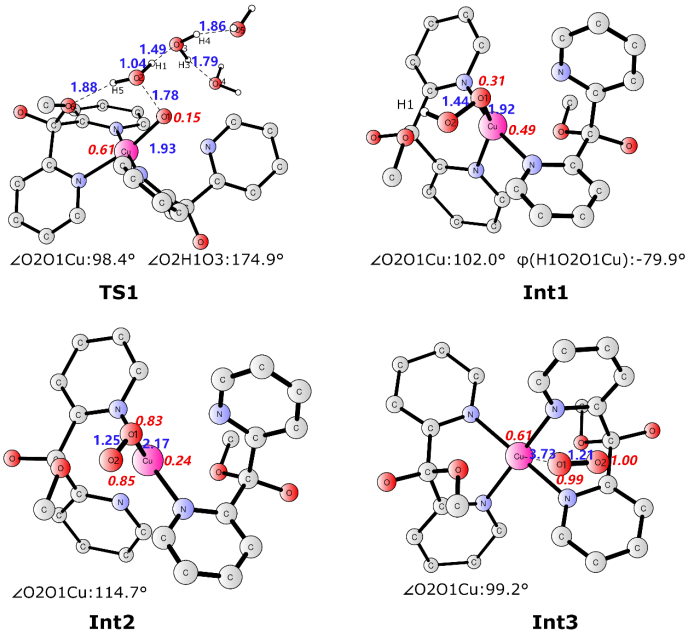

Figure 3. Optimized structure of **TS1** (doublet), **Int1** (doublet), **Int2** (triplet) and **Int3** (quartet). Spin densities on selected atoms are shown in red in italics. Distances are shown in blue in Å. Selected bond angles and dihedral angles are also shown. Unimportant H atoms are not shown.

3 is the active species to trigger the O-O bond formation via water nucleophilic attack mechanism, as is suggested by previous studies.

[42, 43] One water molecule attacks the O1 atom, accompanied by the transfer of one of the protons to the water solution. The located transition state (**TS1**) is displayed in Figure **3**. **TS1** prefers to be a doublet. Spin crossing from quartet to doublet is a prerequisite for the O-O bond formation. **TS1** has only one imaginary frequency of 337.38*i* cm^{-1}, corresponding to the formation of the O1-O2 bond as well as the break of the O2-H1 bond. In this process, the water molecule works as the proton acceptor. The spin densities of Cu and O1 are 0.61 and 0.15, respectively. This suggests that the attacking water provides a pair of electrons to form the σ_{O-O} bond during the O-O bond formation process. In **TS1**, the Cu-O1, O1-O2, and O3-H1 were calculated to be 1.93 Å, 1.78 Å, and 1.49 Å, respectively. The distance of 1.88 Å between H5 (the second proton of the attacking water) and O6 (the oxygen atom of the ligand) indicates the intramolecular hydrogen bonding interaction in **TS1**. The total barrier is 19.3 kcal/mol (Figure **2**) when the energy penalty of the generation of **3** was considered.

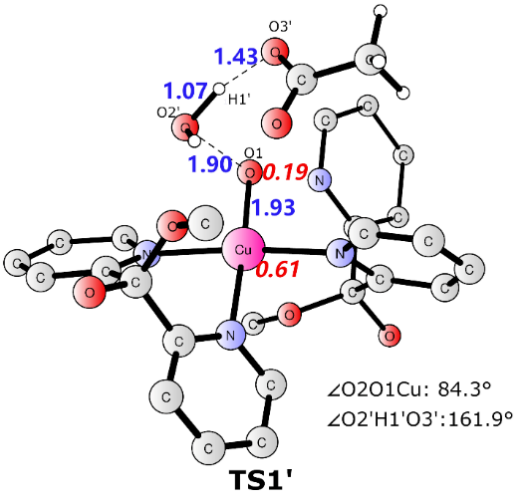

Figure 4. Optimized structure of **TS1** (doublet). Spin densities on selected atoms are shown in red in italics. Distances are shown in blue in Å. Selected bond angles are also shown. Unimportant H atoms are not shown.

The alternative mechanism of the O-O bond formation was also investigated, where the acetate ion from the solution behaves as the proton acceptor. The optimized transition state (TS1') is shown in Figure 4. TS1' is a doublet. The only imaginary frequency of 425.96 *i* cm^{-1} represents to the O1-O2' bond formation and the broken of the O2'-H1' bond. In TS1', the nascent O1-O2' has a distance of 1.90 Å. The calculated distances of Cu-O1, O2'-H2' and H1'-O3' are 1.93, 1.07 and 1.43 Å, respectively. The spin densities on Cu and O1 are 0.61 and 0.16 respectively. The barrier of O-O bond formation via TS1' was calculated to be 21.6 kcal/mol, which is 2.3 kcal/mol higher than the previous pathway.(Figure 3) The present calculations indicate that the water molecule is a better proton acceptor compared with the acetate ion.

Downhill from **TS1**, the hydrogen-peroxide intermediate (**Int1**, **Figure 3**) generates. **Int1** is a doublet, while the quartet state is much higher than the doublet state, lying at +45.6 kcal/mol above the ground state. The O1-O2 has a distance of 1.44 Å. The Cu-O1 distance was calculated to be 1.92 Å. The spin densities on Cu and O1 are 0.49 and 0.31, respectively. The formation of **Int1** from **3** is exergonic by 23.1 kcal/mol.

From **Int1**, a PCET process leads to the generation of the superoxide intermediate (**Int2**, Figure 3) associated with a redox potential of -0.03 V. **Int2** is a triplet. In **Int2**, the Cu-O1 and O1-O2 distances became 2.17 Å and 1.25 Å, respectively. The spin density on Cu, O1, and O2 are 0.24, 0.83, and 0.85, respectively. **Int2** undergoes another one-electron oxidation process, resulting in **Int3** (**Figure 3**). In **Int3**, the triplet O_2 has already formed. As displayed in **Figure 3**, O1-O2 has a distance of 1.21 Å. The spin densities on O1 and O2 are 0.99 and 1.00, respectively. After the oxidation of **Int2**, the O_2 is released from the copper center, and the Cu-O1 distance was calculated to 3.73 Å. The redox potential of this oxidation process was calculated to be -0.32 V, which means that the disclosure of the O_2 is quite facile.

From **Figure 2**, it is clear that the O-O bond formation has the highest barrier, which is 19.3 kcal/mol. The calculated barrier was slightly overestimated compared to the experimentally reported TOF of 9.20 s^{-1}, which corresponds to a total barrier of 16.1 kcal/mol. [34] The oxidation processes contribute to the total barrier, as evidenced by the energy profile. Electron-donation groups facilitate the oxidation processes, which would decrease the total barrier of the catalytic cycle. The calculated redox potential for **1-H_2O/2** and **2/3** are higher than the reference potential. One thing that should be discussed is whether **3** can be obtained or not. The occurrence of the irreversible chemical reaction of the O-O bond formation following the formation of **3** and the reasonable barrier of the catalytic cycle suggests that **3** is a possible intermediate in the catalytic process. [45] The catalytic cycle is shown in **Figure 5**.

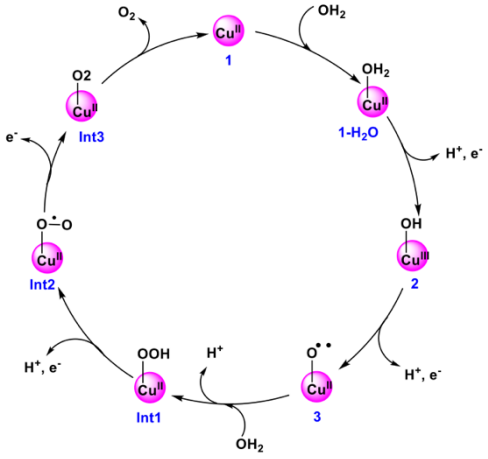

Figure 5. Suggested catalytic cycle for the water oxidation reaction.

The barrier for the water oxidation at pH = 7.81 with an applied potential of 1.5 V was calculated to be 11.4 kcal/mol higher than that at pH = 11.4. (**Figure S3**) The increase in the barrier is attributed to the increased oxidation potential of the initial two oxidation steps. The increased barrier provides a plausible explanation for the experimental finding that the catalytical rate is 32.9 times faster at pH = 11.84 than at pH = 7.81. [34] The 11.4 kcal/mol barrier difference is overestimated compared with the calculated TOF difference at different pH conditions. The calculation shows that the higher reaction pH leads to improved catalytically efficiency for the water oxidation reaction, in which the proton release involved oxidation steps contribute to the total energy barrier.

Alternative transition metal, such as Mn, Fe and Co may potentially substitute the copper center as viable water oxidation catalysts. The corresponding calculated redox potentials and O-O bond formation barriers are summarized in Table **1**. Figure 6 presents the constructed energy diagram. The Cu-based water oxidation catalyst (Cu-WOC) exhibits the highest oxidation potential for the

first PCET process. Among the evaluated complexes, the oxidation of Mn^{II} to Mn^{III} is the most thermodynamically favorable pathway with the lowest oxidation potential of 0.66 V. All possible catalysts have qualitatively comparable oxidation potential values (around 1.6 V) for the second PCET process. The O-O bond formation triggered by the Cu^{IV} intermediate has the lowest barrier of 3.7 kcal/mol, corresponding to a total barrier of 19.3 kcal/mol. Notably, two PCET processes for Co-WOC were calculated to be 1.25 V and 1.52V, respectively, and the O-O bond formation has a barrier of 15.2 kcal/mol. These computational results suggest that Co based complex could be a promising candidate for water oxidation catalysis, though experimental validation remains necessary.

Table 1. Calculated redox potentials and total barriers for different metal based complexes.

	Redox potentials		The barrier of O-O bond formation in kcal/mol
	III/II in V	IV/III in V	
Cu-WOC	1.72	1.65	3.7
Mn-WOC	0.66	1.80	28.3
Fe-WOC	0.65	1.61	24.5
Co-WOC	1.25	1.53	15.2

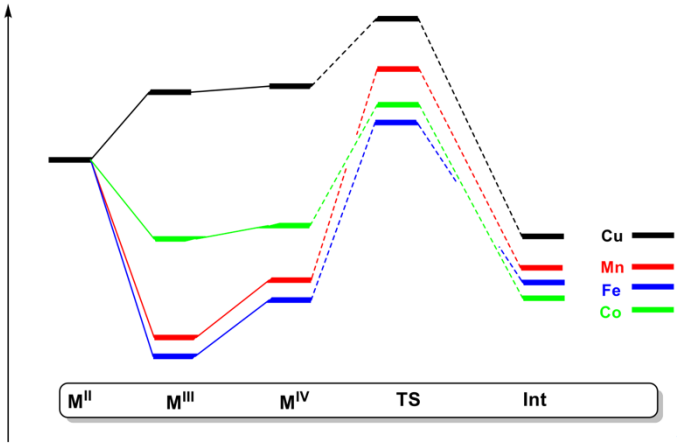

Figure 6. Energy diagram for water oxidation catalyzed by different metal based complexes. The dark line for Cu, red line for Mn, blue line for Fe and green line for Co.

4. Conclusion

The mechanism of water oxidation reaction catalyzed by a mononuclear Cu-based complex was investigated in the present work. The density functional theory calculations show that only one water can coordinate with the Cu^{II} center before the occurrence of a water oxidation reaction. After two subsequent PCET processes of **1-H_2O** (Cu^{II}-H_2O), a Cu^{II}-oxygen diradical species (**3**) is generated. **3** triggers the O-O bond formation via the water nucleophilic attack mechanism, during which water molecules behave as the proton acceptor. The triplet O_2 molecule can be released after two oxidation processes from **Int1**. Two OH groups keep the protonation state during the catalytic cycle. The O-O bond formation is the rate-determining step associated with a total barrier of 19.3 kcal/mol. A series of alternative transition metal complexes (Mn, Fe, Co) were also investigated. The calculation results suggest that Co based complex could be a promising water oxidation catalyst.

Supporting information

The online version contains supplementary material available at website.
https://global-sci.com/storage/self-storage/cicc-2025-49-1-r1-si.pdf

Acknowledgements

This work was supported by startup funding from Zhengzhou Normal University (2021-702449), the Natural Science Foundation of Henan Province (232300420409), Key Scientific Research Projects of Colleges and Universities in Henan Province (24B530006), and Scientific and technological project of Henan Province (242102230183).

References

[1] Berardi S., Drouet S., Francas L., Gimbert-Surinach C., Guttentag M., Richmond C., Stoll T., Llobet A. Molecular artificial photosynthesis. *Chem. Soc. Rev.*, **43** (2014), 7501-7519.

[2] Li J., Triana C.A., Wan W., Adiyeri Saseendran D.P., Zhao Y., Balaghi S.E., Heidari S., Patzke G.R. Molecular and heterogeneous water oxidation catalysts: recent progress and joint perspectives. *Chem. Soc. Rev.*, **50** (2021), 2444-2485.

[3] Gersten S.W., Samuels G.J., Meyer T.J. Catalytic oxidation of water by an oxo-bridged ruthenium dimer. *J. Am. Chem. Soc.*, **104** (1982), 4030-4032.

[4] Liu T., Zhan S., Shen N., Wang L., Szabo Z., Yang H., Ahlquist M.S.G., Sun L. Bioinspired active site with a coordination-adaptive organosulfonate ligand for catalytic water oxidation at neutral pH. *J. Am. Chem. Soc.*, **145** (2023), 11818-11828.

[5] Ma H.-C., Hsiao S.-C., Wang Y.-H. Tuning primary and secondary coordination spheres of ruthenium complexes for the homogeneous water oxidation reaction: a perspective from catalytic activity and overpotential. *Catal. Sci. Technol.*, **13** (2023), 1598-1622.

[6] Noll N., Krause A.-M., Beuerle F., Würthner F. Enzyme-like water preorganization in a synthetic molecular cleft for homogeneous water oxidation catalysis. *Nat. Catal.*, **5** (2022), 867-877.

[7] Hull J.F., Balcells D., Blakemore J.D., Incarvito C.D., Eisenstein O., Brudvig G.W., Crabtree R.H. Highly active and robust Cp* iridium complexes for catalytic water oxidation. *J. Am. Chem. Soc.*, **131** (2009), 8730-8731.

[8] Gil-Sepulcre M., Llobet A. Molecular water oxidation catalysts based on first-row transition metal complexes. *Nat. Catal.*, **5** (2022), 79-82.

[9] Wei X.Z., Ding T.Y., Wang Y., Yang B., Yang Q.Q., Ye S., Tung C.H., Wu L.Z. Tracking an Fe(V)(O) intermediate for

water oxidation in water. *Angew. Chem. Int. Ed.*, **62** (2023), e202308192.

[10] Zhang H.T., Guo Y.H., Xiao Y., Du H.Y., Zhang M.T. Heterobimetallic NiFe cooperative molecular water oxidation catalyst. *Angew. Chem. Int. Ed.*, **62** (2023), e202218859.

[11] Pahar S., Maayan G. An intramolecular cobalt-peptoid complex as an efficient electrocatalyst for water oxidation at low overpotential. *Chem. Sci.*, **15** (2024), 12928-12938.

[12] Li G., Ahlquist M. O-O bond formation via radical coupling in a dinuclear iron water oxidation catalyst with high catalytic activity. *Dalton Trans.*, (2024).

[13] Huang Q., Chen J., Luan P., Ding C., Li C. Understanding the factors governing the water oxidation reaction pathway of mononuclear and binuclear cobalt phthalocyanine catalysts. *Chem. Sci.*, **13** (2022), 8797-8803.

[14] Xie F., Zhang M.-T. Bimetallic water oxidation: one-site catalysis with two-sites oxidation. *J. Energy Chem.*, **63** (2021), 1-7.

[15] Liu C., Bos D., Hartog B., Meijer D., Ramakrishnan A., Bonnet S. Ligand controls the activity of light-driven water oxidation catalyzed by nickel(ii) porphyrin complexes in neutral homogeneous aqueous solutions. *Angew. Chem. Int. Ed.*, **60** (2021), 13463-13469.

[16] Chen Q.F., Xian K.L., Zhang H.T., Su X.J., Liao R.Z., Zhang M.T. Pivotal role of geometry regulation on O-O bond formation mechanism of bimetallic water oxidation catalysts. *Angew. Chem. Int. Ed.*, (2024), e202317514.

[17] Santoni M.P., La Ganga G., Nardo V.M., Puntoriero F., Campagna S. Use of a vanadium species as a catalyst in photoinduced water oxidation. *J. Am. Chem. Soc.*, **136** (2014), 8189-8192.

[18] Li Y., Yao R., Chen Y., Xu B., Chen C., Zhang C. Mimicking the catalytic center for the water-splitting reaction in photosystem II. *Catalysts*, **10** (2020), 185.

[19] Maayan G., Gluz N., Christou G. Bioinspired soluble manganese cluster as a water oxidation electrocatalyst with low overpotential. *Nat. Catal.*, **1** (2018), 48-54.

[20] Liao R.-Z., Siegbahn P.E.M. Quantum chemical modeling of homogeneous water oxidation catalysis. *ChemSusChem*, **10** (2017), 4236-4263.

[21] Schilling M., Luber S. Computational modeling of cobalt-based water oxidation: current status and future challenges. *Front. Chem.*, **6** (2018), 1-21.

[22] Li Y.Y., Liao R.Z. Exploring the cooperation of the redox non-innocent ligand and di-cobalt center for the water oxidation reaction catalyzed by a binuclear complex. *ChemSusChem*, **17** (2024), e202400123.

[23] Wu P., Yan S., Fang W., Wang B. Molecular mechanism of the mononuclear copper complex-catalyzed water oxidation from cluster-continuum model calculations. *ChemSusChem*, (2022), e202102508.

[24] Hu S., Xu P., Xu R.X., Zheng X. Unveiling the high catalytic activity of a dinuclear iron complex for the oxygen evolution reaction. *Inorg. Chem.*, **60** (2021), 7297-7305.

[25] Li M., Liao R.Z. Water oxidation catalyzed by a bioinspired tetranuclear manganese complex: mechanistic study and prediction. *ChemSusChem*, **15** (2022), e202200187.

[26] Sproviero E.M. DFT/B3LYP study of the mechanisms of the O2 formation reaction catalyzed by the $[(terpy)(H_2O)Mn^{III}(O)_2Mn^{IV}(OH_2)(terpy)](NO_3)_3$ complex: a paradigm for photosystem II. *J. Inorg. Biochem.*, **171** (2017), 52-66.

[27] de Gracia Triviño J.A., Ahlquist M.S.G. Operando condition reaction modeling shows highly dynamic attachment of oligomeric ruthenium catalysts. *ACS Catal.*, **13** (2023), 1270-1279.

[28] Pan H., Duan L., Liao R.Z. Capturing the role of phosphate in the Ni-PY5 catalyzed water oxidation. *ChemCatChem*, **12** (2019), 219-226.

[29] Li Y.Y., Wang X.Y., Li H.J., Chen J.Y., Kou Y.H., Li X., Wang Y. Theoretical study on the mechanism of water oxidation catalyzed by a mononuclear copper complex: important roles of a redox non-innocent ligand and HPO_4^{2-} anion. *RSC Adv.*, **13** (2023), 8352-8359.

[30] Gorantla K.R., Mallik B.S. Mechanistic insight into the O2 evolution catalyzed by copper complexes with tetra- and pentadentate ligands. *J. Phys. Chem. A*, **125** (2021), 6461-6473.

[31] Siegbahn P.E.M. Theoretical study of O_2 reduction and water oxidation in multicopper oxidases. *J. Phys. Chem. A*, **124** (2020), 5849-5855.

[32] Mao Q.-Y., Pang Y.-J., Li X.-C., Chen G.-J., Tan H.-W. Theoretical study of the mechanisms of two copper water oxidation electrocatalysts with bipyridine ligands. *ACS Catal.*, **9** (2019), 8798-8809.

[33] Funes-Ardoiz I., Garrido-Barros P., Llobet A., Maseras F. Single electron transfer steps in water oxidation catalysis: redefining the mechanistic scenario. *ACS Catal.*, **7** (2017), 1712-1719.

[34] Shi N.-N., Xie W.-J., Zhang D.-M., Fan Y.-H., Cui L.-S., Wang M. Mononuclear copper complex as bifunctional electrocatalyst for CO_2 reduction and water oxidation. *J. Electroanal. Chem.*, **886** (2021), 115106.

[35] Frisch M.J. et al. Gaussian 16, Revision C.01., Gaussian Inc., Wallingford CT, 2016.

[36] Becke A.D. Density-functional thermochemistry. III. The role of exact exchange. *J. Chem. Phys.*, **98** (1993), 5648-5652.

[37] Grimme S. Density functional theory with London dispersion corrections. *WIREs Comput. Mol. Sci.*, **1** (2011), 211-228.

[38] Andrae D., Häußermann U., Dolg M., Stoll H., Preuß H. Energy-adjusted *ab initio* pseudopotentials for the second and third row transition elements. *Theor. Chim. Acta*, **77** (1990), 123-144.

[39] Marenich A.V., Cramer C.J., Truhlar D.G. Universal solvation model based on solute electron density and on a continuum model of the solvent defined by the bulk dielectric constant and atomic surface tensions. *J. Phys. Chem. B*, **113** (2009), 6378-6396.

[40] Isse A.A., Gennaro A. Absolute potential of the standard hydrogen electrode and the problem of interconversion of potentials in different solvents. *J. Phys. Chem. B*, **114** (2010), 7894-7899.

[41] Camaioni D.M., Schwerdtfeger C.A. Comment on "Accurate experimental values for the free energies of hydration of H^+, OH^-, and H_3O^+". *J. Phys. Chem. A*, **109** (2005), 10795-10797.

[42] Chen Q.F., Cheng Z.Y., Liao R.Z., Zhang M.-T. Bioinspired trinuclear copper catalyst for water oxidation with a turnover frequency up to 20000 s^{-1}. *J. Am. Chem. Soc.*, **143** (2021), 19761-19768.

[43] Fan Q., Li M., Wang C., Wang G., Kong X., Zhu Q. Deciphering the active species and reaction mechanism in

water oxidation catalyzed by a copper complex with redox-active ligands. *Inorg. Chem. Front.*, **11** (2024), 2365-2372.

[44] Li Y.Y., Ke Y., Siegbahn P.E.M., Liao R.Z. Mechanism of water oxidation catalyzed by a mononuclear manganese complex. *ChemSusChem*, **10** (2017), 903-911.